Quantum Evolution in One Dimensional Disordered Systems: Localisation and Oscillations

Edward Sharp*[1]

Project Advisor: Francisco González Montoya†[1]

[1]School of Mathematics, University of Bristol, Fry Building, Woodland Road, Bristol, BS8 1UG, United Kingdom.

Abstract

This work is a simple example of the quantum dynamics of a particle in a disordered system in one dimension. In particular, we illustrate numerically the phenomenon of Anderson localisation of a wave packet using a basic model constructed with small random rectangular potential barriers. Also, we study the dynamics of a quantum particle in a disordered potential formed by an harmonic oscillator perturbed by random rectangular barriers. To show the effects of disorder on the dynamics of the system, we compare the time evolution of the wave function of the unperturbed harmonic oscillator with the wave function of the disordered system. We do this by taking the scalar product between the unperturbed and perturbed wave functions at each timestep for different values of the perturbation parameters affecting the disordered wave packet.

*yx18110@bristol.ac.uk, emgsharp@gmail.com

†f.gonzalez.montoya@protonmail.com

1 Introduction

Quantum disordered systems are common in nature and are very important in applications. In particular, the study of the evolution and transport phenomenon in disordered potentials is a relevant problem related to electron conduction, light propagation, chemical reactions, and so on. A general discussion about transport in disordered systems is found in the recent review article [1].

One of the most intriguing properties of disordered systems is the absence of diffusion of wave packets in the space for some special cases. This peculiar phenomenon is called Anderson localisation [2, 3] and it is a consequence of the interference of the waves that are transmitted and reflected in the disordered media. The localisation lengths of the wave functions are related with the dimension of the system and the properties of the disorder.

A simple model has been proposed to study transport properties of wave function of disordered potentials in one dimension, see [4]. In this model, the total potential energy consists of a sequence of rectangular barriers with the same width and random height. The energy of the particle considered is larger than the maximal value of the potential energy. The analytical solutions of the Schrödinger equation for this kind of system can be constructed using the elementary solutions of the wave equation for the step barrier potential with finite width. With these solutions it is possible to obtain analytical expressions for the transmission and reflection coefficients and study the transport in the system.

In the present work, we present two basic numerical examples to illustrate the quantum evolution of a particle in a disordered one dimensional potential. These examples are aimed at helping the undergraduate university student better understand how seemingly simple quantum mechanical effects can lead to interesting phenomena. The outline for this work is the following: in section 2, we explain the Anderson localisation phenomenon using solutions to the time-independent Schrödinger equation for a series of step barriers. In section 3, we investigate the time evolution of the wave function for a particle in a free particle potential and also a harmonic oscillator potential, both of which are perturbed by adding disorder at a number of points. To appreciate the effects of the disorder on the temporal evolution of the system we consider different values of the parameters of the potential barriers that form the perturbation. Finally, we present our conclusions and remarks in section 4.

2 Transfer matrices and Anderson localisation

The general solution of the Schrödinger wave equation for a particle in a finite rectangular step barrier is well known, see for example [5]. Based on this elementary solution is possible to construct the solution of more complex systems like the following. Let us consider a potential energy V formed by arbitrary $N \in \mathbb{N}$ step functions with random height in each region. In each of these regions, we solve the one-dimensional time-independent Schrödinger equation,

$$-\frac{\hbar^2}{2m}\frac{d^2}{dx^2}\Psi_j(x) + V_j\Psi(x) = E\Psi_j(x), \tag{1}$$

where $V_j(x)$ is the constant potential in region $j \in \mathbb{N}, 1 \leq j \leq N$. This gives the solutions in the j^{th} and $(j+1)^{th}$ regions,

$$\Psi_j = A_j e^{ik_j x} + B_j e^{-ik_j x}, \tag{2}$$

$$\Psi_{j+1} = C_{j+1} e^{ik_{j+1} x} + D_{j+1} e^{-ik_{j+1} x} \tag{3}$$

where A_j, C_{j+1} are the coefficients for right moving components of the wave function, B_j, D_{j+1} are the coefficients for the left moving components of the wave function and $k_j = \sqrt{2m(E - V_j)}/\hbar$.

At this point, we would like a relation between the coefficients A_j and B_j for the incident wave, and C_{j+1} and D_{j+1} for the transmitted wave at each step. We would like this to be of the form,

$$\begin{pmatrix} A_j \\ B_j \end{pmatrix} = \boldsymbol{p}_j \begin{pmatrix} C_{j+1} \\ D_{j+1} \end{pmatrix}, \tag{4}$$

where $\boldsymbol{p}_j$ is the 2x2 propagation matrix at step j. In this way we can calculate the probability that a particle is transmitted over the whole potential by using a product of propagation matrices.

By requiring that Ψ_j and $\frac{d\Psi_j}{dx}$ are continuous functions at the boundaries between regions and using Eq. (2) and Eq. (3), we find that at each step:

$$\boldsymbol{p}_j = \frac{1}{2} \begin{pmatrix} 1 + \frac{k_{j+1}}{k_j} & 1 - \frac{k_{j+1}}{k_j} \\ 1 - \frac{k_{j+1}}{k_j} & 1 + \frac{k_{j+1}}{k_j} \end{pmatrix}. \tag{5}$$

The transfer matrix for region j is given by Eq. (5), which leads us to the total transfer matrix,

$$\boldsymbol{P} = \prod_{j=1}^{N} \boldsymbol{p}_j. \tag{6}$$

Assuming that particle is incident from the left, we have that $A_1 = 1$ and $D_N = 0$, hence,

$$\begin{pmatrix} A_1 \\ B_1 \end{pmatrix} = \begin{pmatrix} 1 \\ B_1 \end{pmatrix} = \boldsymbol{P} \begin{pmatrix} C_N \\ D_N \end{pmatrix} = \boldsymbol{P} \begin{pmatrix} C_N \\ 0 \end{pmatrix} \tag{7}$$

Finally, we can see that since $1 = P_{11}C$, the transmission probability is given by the equality,

$$|C|^2 = \frac{1}{|P_{11}|^2}, \tag{8}$$

where P_{11} is the top-left entry Eq. (6).

For the sake of simplicity, let us consider a particle with momentum positive and only a potential barrier like in Figure 1a. Part of the wave function is transmitted through the potential barrier and other part is reflected by barrier. The probability to find the particle in a given position x changes due to the effect of the barrier. If the particle has more energy E then the effect of the barrier is less noticeable. If we increase the number of barriers, the effects accumulate and the probability to find the particle on the right side decreases. However, if the energy of the particle E is bigger than the height of the barriers then the situation is more complex. The transmitted and reflected waves could interfere with each other and thus generate the localisation phenomenon. This time-independent scenario is indicative of the cancellation effect which is key to understanding Anderson localisation. Time-dependent simulations are more complex, requiring numerical methods to solve the Schrödinger equation.

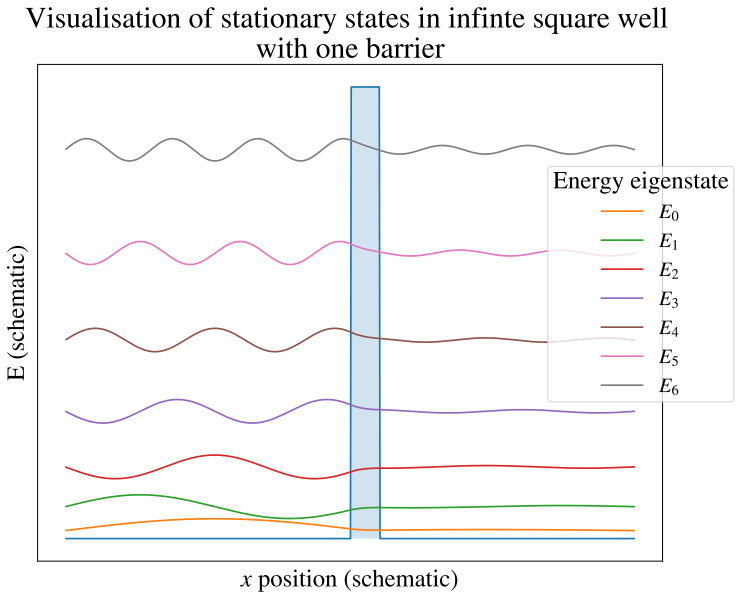

(a) Solution to the Schrödinger equation for a single barrier. We notice that the wave function oscillates as expected in areas where the potential is zero, and decays exponentially in areas where the potential is bigger than the height of the barrier.

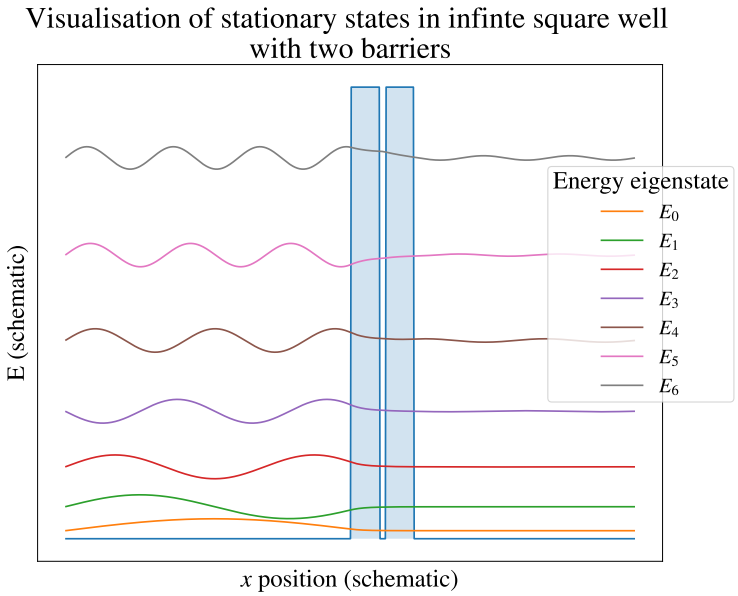

(b) Solution of the Schrödinger equation for a double barrier. The second barrier has caused the wave function to oscillate with less amplitude in the right region when compared to the single barrier case.

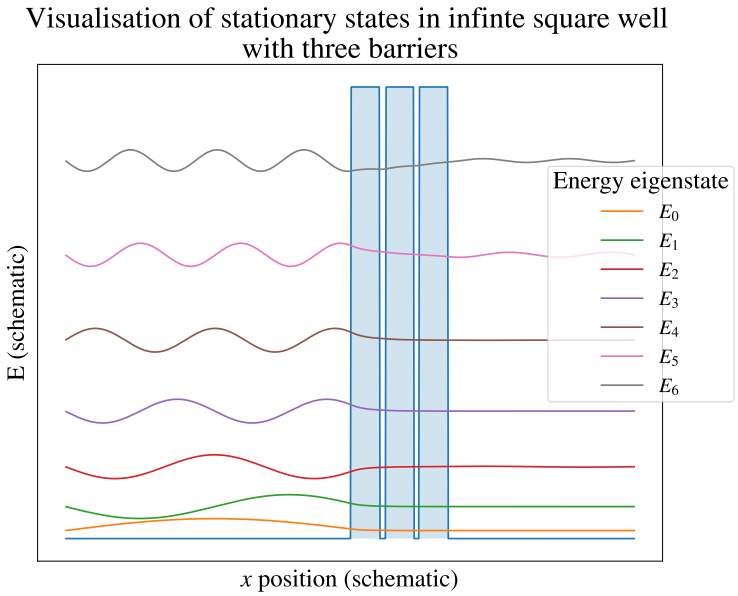

(c) Solution of the Schrödinger equation for a triple barrier.

Figure 1: The figures indicate the reduction in the probability that a wave is transmitted when the number of barriers is increased. In (a) we see that transmission is seriously impeded for lower energies, but not so much for higher energies. This contrasts with (c), where we see that for waves with energies below E_4 transmission is almost completely stopped, and is seriously lowered for all energies.

3 Anderson localisation

The process of understanding how a Gaussian wave packet evolves in time is made simpler by direct visualisation of the systems involved. In order to serve this purpose, we have developed an intuitive tool for generating animations of disordered quantum systems, where a wave is subjected to a user-defined potential. Our code makes use of the Crank-Nicolson method (see appendix A) for numerically estimating the time evolution of a quantum system. The simulation tool is free to access via our GitHub repository online (see appendix B).

In order to illustrate numerically the Anderson localisation phenomenon generated by a disordered potential energy let us consider an initial wave packet in a potential energy formed by an array of rectangular potential barriers similar to the work in [4]. A potential landscape, spanning from $-a$ to a, is discretised into N rectangular barriers of width $l_c = \frac{2a}{N}$. The height of each barrier is a small number V_j, where $j = 1, ..., N$. Each V_j is drawn uniformly at random such that $V_j \sim \text{Uniform}[-\varepsilon, \varepsilon]$, where ε is the disorder parameter with units of energy. There is also the ability to add spacing between the disordered points using a spacing parameter, s, which has units of length. The spacing parameter s works by acting on the perturbation V_j as follows

$$V_j = \begin{cases} V_j, & \text{if } j \bmod s = 0 \\ 0, & \text{otherwise,} \end{cases}$$

if $s > 0$ and $V_j = V_j \; \forall j$ if $s = 0$, where $j = 1, ..., N$. A Gaussian curve with the equation:

$$\Psi(x) = \frac{1}{\sqrt[4]{2\pi\sigma_0^2}} \exp\left(\frac{-(x - x_0)^2}{4\sigma_0^2}\right) \exp\left(ik_0 x\right), \tag{9}$$

is then added to this landscape in order for us to analyse its time evolution.

3.1 Free particle

For the following simulations we choose the initial parameters $N = 150$, $x_0 = 0$, $\sigma_0 = 1.5$ and $k_0 = 3.0$, which represent the initial position, initial shape and initial momentum of the wave, respectively. After some sufficiently long time $\tau \approx 5$, we take an snapshot of the wave packet $\Psi(x, \tau)$ of the particle, which can be seen in Figure 2. We can appreciate how the wave packet $\Psi(x, \tau)$ is confined in some finite region of space, and that the length of the region of localisation decreases as the value of ε is increased.

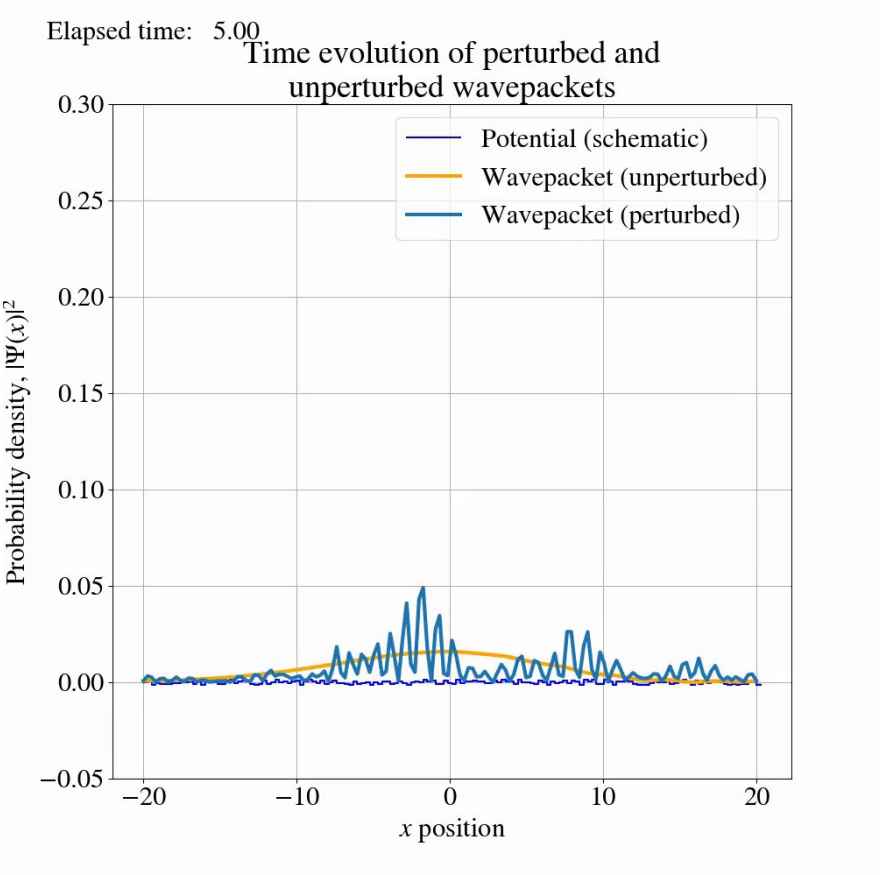

(a) Disorder, $\varepsilon = 0.1$.

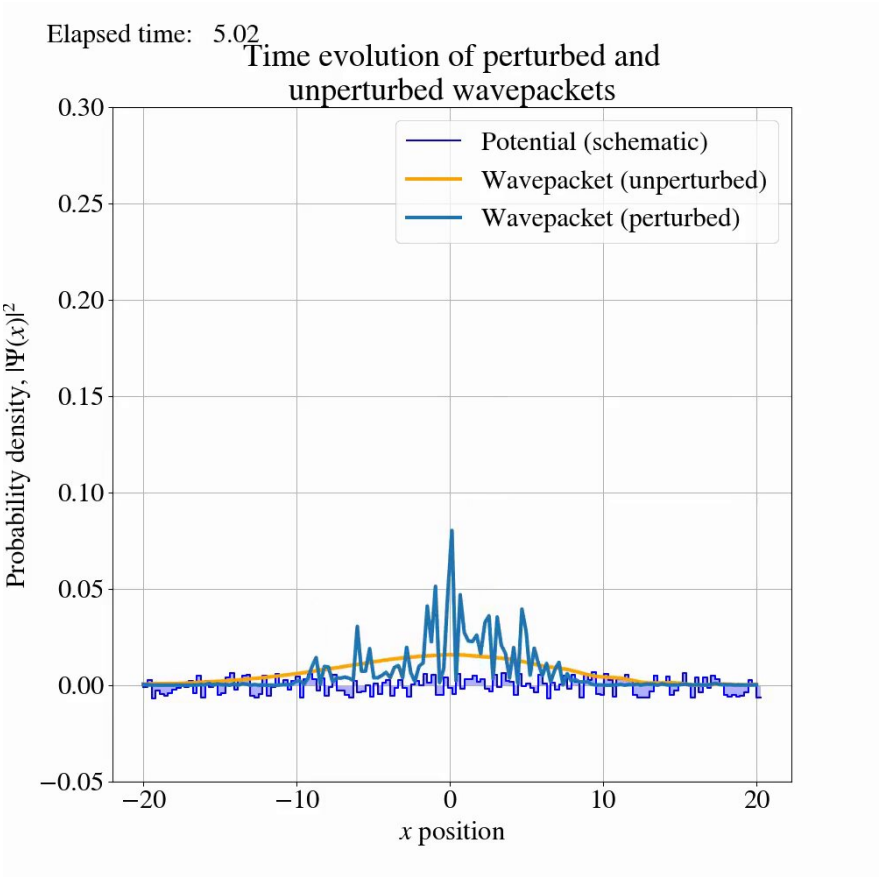

(b) Disorder, $\varepsilon = 0.5$.

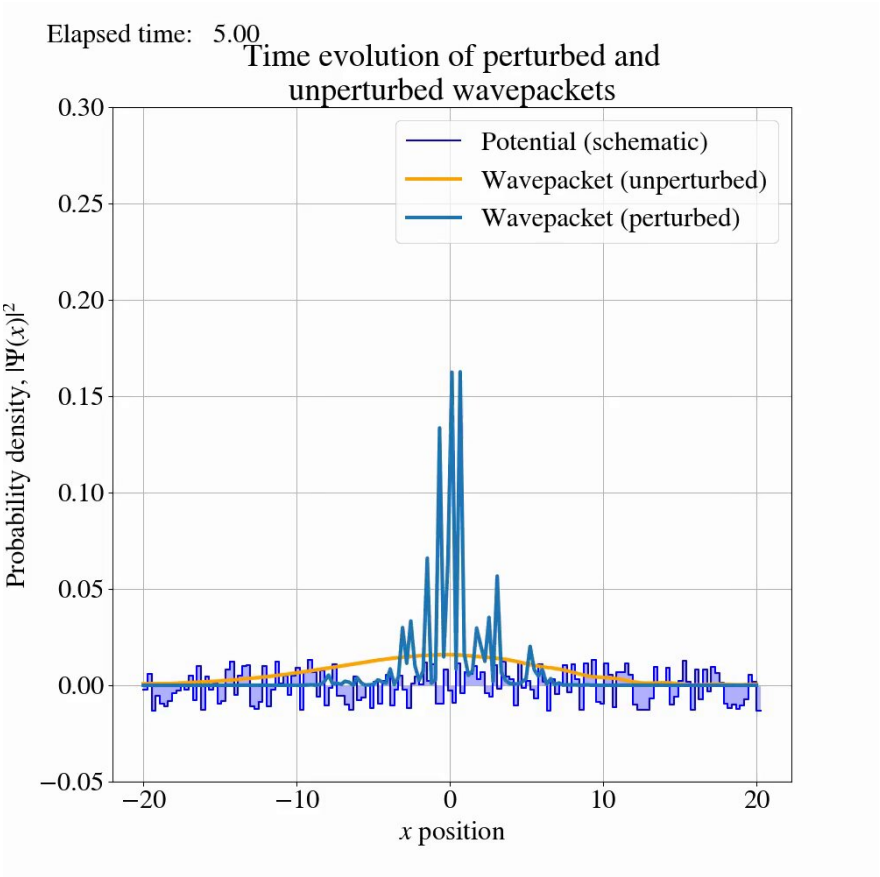

(c) Disorder, $\varepsilon = 1.0$.

Figure 2: Plots showing the Anderson localisation of a wave function $\Psi(x, \tau)$, $\tau \approx 5$, for different values of the the maximal value of the disorder to the potential $\varepsilon = 0.1, 0.5, 1.0$. It is clear to see that as the disorder increases, the particle is localised in a narrower region of the space.

3.2 Noisy harmonic oscillator

We now consider the effect of disorder on the motion of a wave through a harmonic oscillator potential. The initial wave function is a Gaussian with the same parameters as in Eq. (9), although we now use $N = 100$ in order to increase the speed of the simulation. The setup code for the oscillator can be found in appendix B. We have varied the maximal amplitude of the barriers that generate the disorder ε, and also the spacing s between barriers in order to study the effect of these factors on the inner product between perturbed and unperturbed waves. By measuring the inner product, we seek to understand how increasing the disorder and spacing affects the difference in phase between the states.

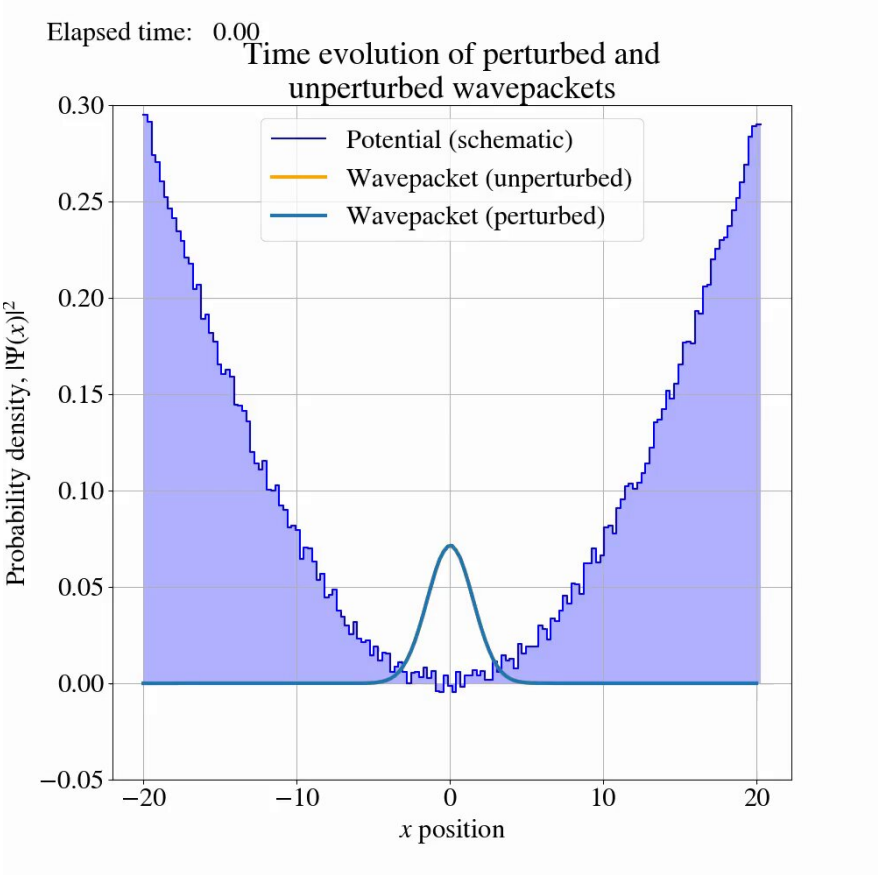

(a) Screenshot at $t = 0$.

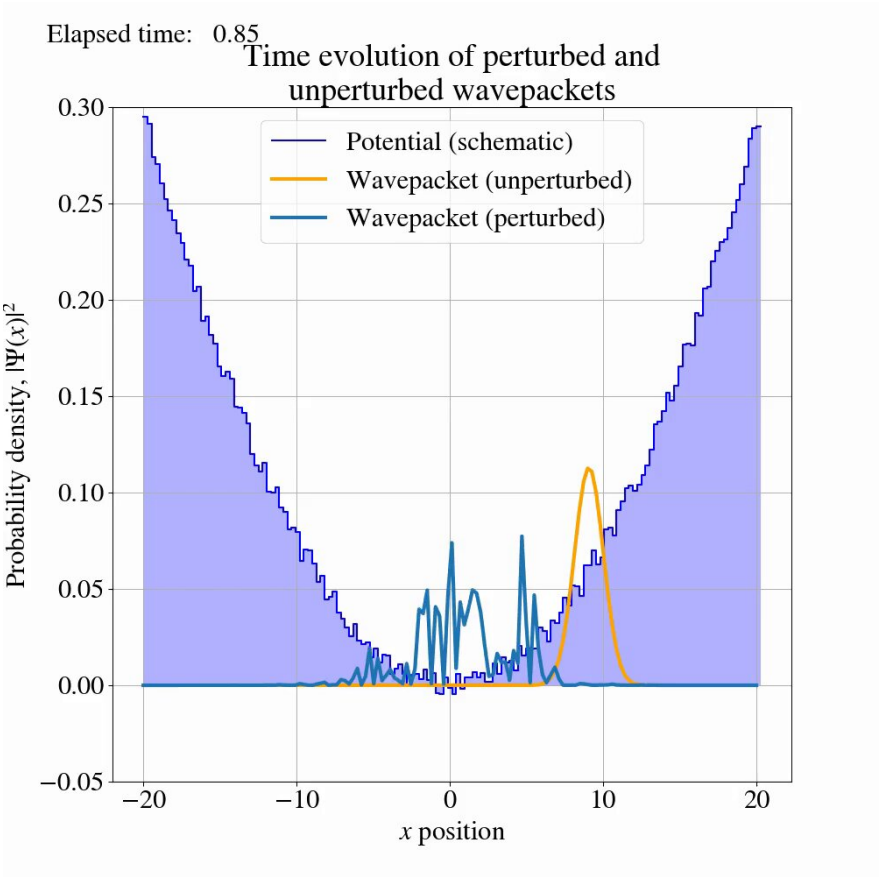

(b) Screenshot at $t = 0.85$ fs.

Figure 3: Snapshots for disordered quantum harmonic oscillator with $\varepsilon = 0.5$ and $s = 0$ at times $t = 0$ and $t = 0.85$. At time $t = 0$, the wave functions are in phase. As time moves on we notice that the perturbed wave function remains localised at the origin whilst the unperturbed wave oscillates normally.

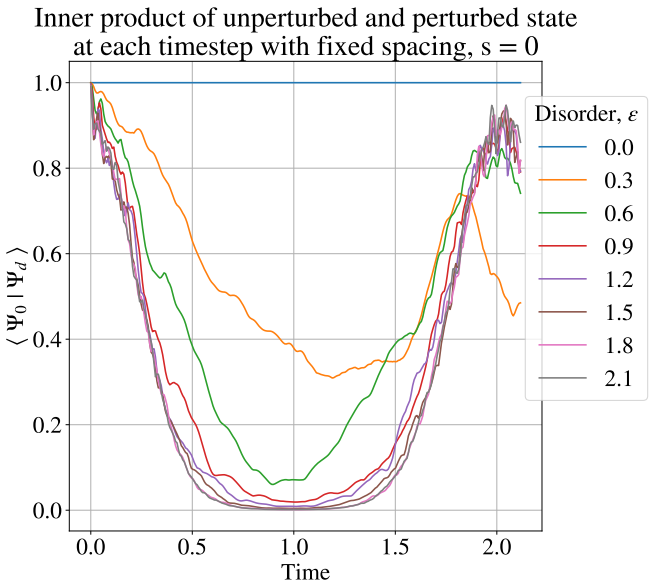

(a) Spacing, $s = 0.0$.

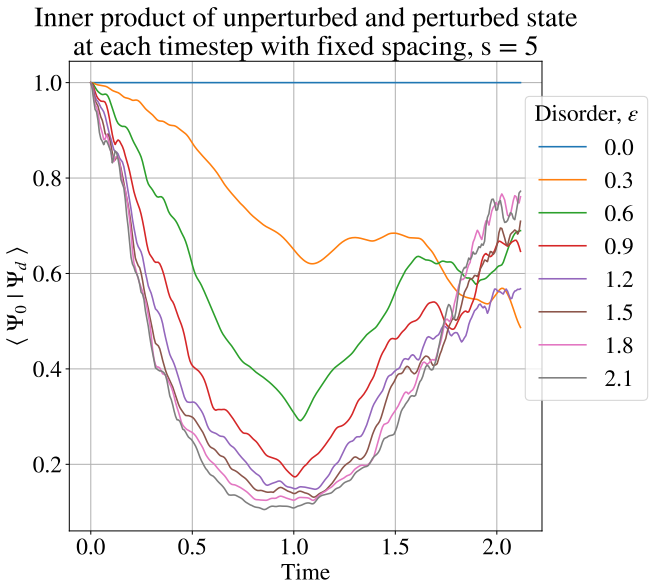

(b) Spacing, $s = 5$.

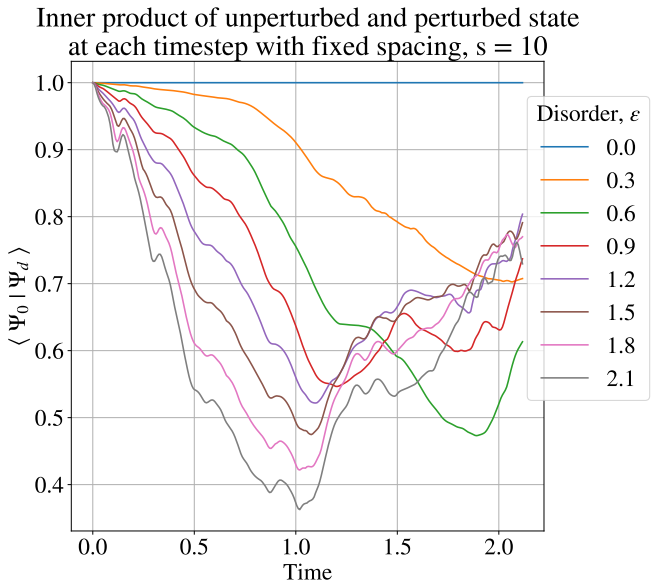

(c) Spacing, $s = 10$.

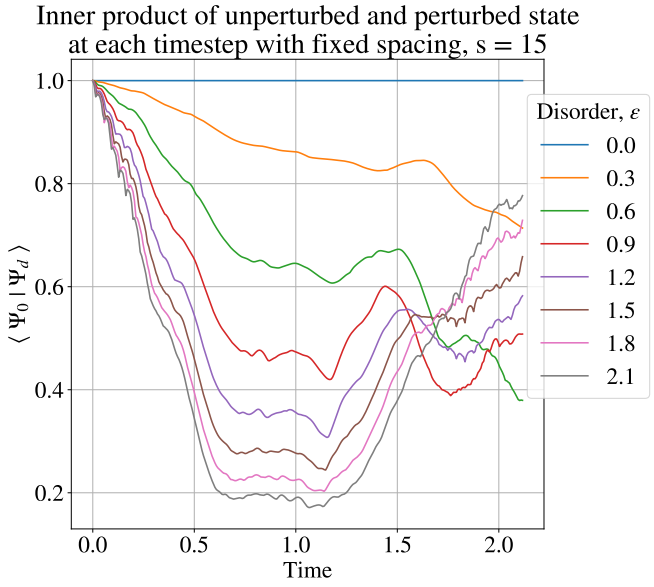

(d) Spacing, $s = 15$.

Figure 4: Plots for the average inner product $\langle \Psi_0(x,t) | \Psi_p(x,t) \rangle$ using different values of step spacing (a) $s = 0$, (b) $s = 5$, (c) $s = 10$, and (d) $s = 15$ as the maximal amplitude of the barriers ε is varied. In each plot we can see that increasing the disorder ε causes the inner product to be lower on average. From (a) we can directly read the period of the wave's oscillation.

We will first consider Figure 4a, in which we have set the spacing $s = 0$, i.e. disorder at every step of the oscillator. As expected, when $\varepsilon = 0$ the inner product remains constant at $\langle \Psi_0(x,t) | \Psi_p(x,t) \rangle = 1$, indicating that the waves stay totally in phase. This is consistent for any value of s. As ε is in-

creased, we see that the waves drift out of phase more quickly. In this case the figure shows that the waves drift completely out of phase and the lines echo the period of oscillation of the waves when ε is high. We also see this in the animation screenshots, where the perturbed wave remains completely localised in the centre for higher values of ε. This is an example of Anderson localisation.

In Figures 4b, 4c and 4d, we increase the spacing to $s = 5$, $s = 10$, and $s = 15$, respectively. We can see that as the spacing is increased, the perturbed wave is less localised, which is indicated by the fact that the inner product $\langle \Psi_0(x,t) | \Psi_p(x,t) \rangle$ approaches 1. This is also expected as fewer disordered points would lead to less localisation.

In Figures 5 and 6, we see that the inner product $\langle \Psi_0(x,t) | \Psi_p(x,t) \rangle$ decreases as the disorder parameter ε is increased and increases as the spacing s between the barriers is increased.

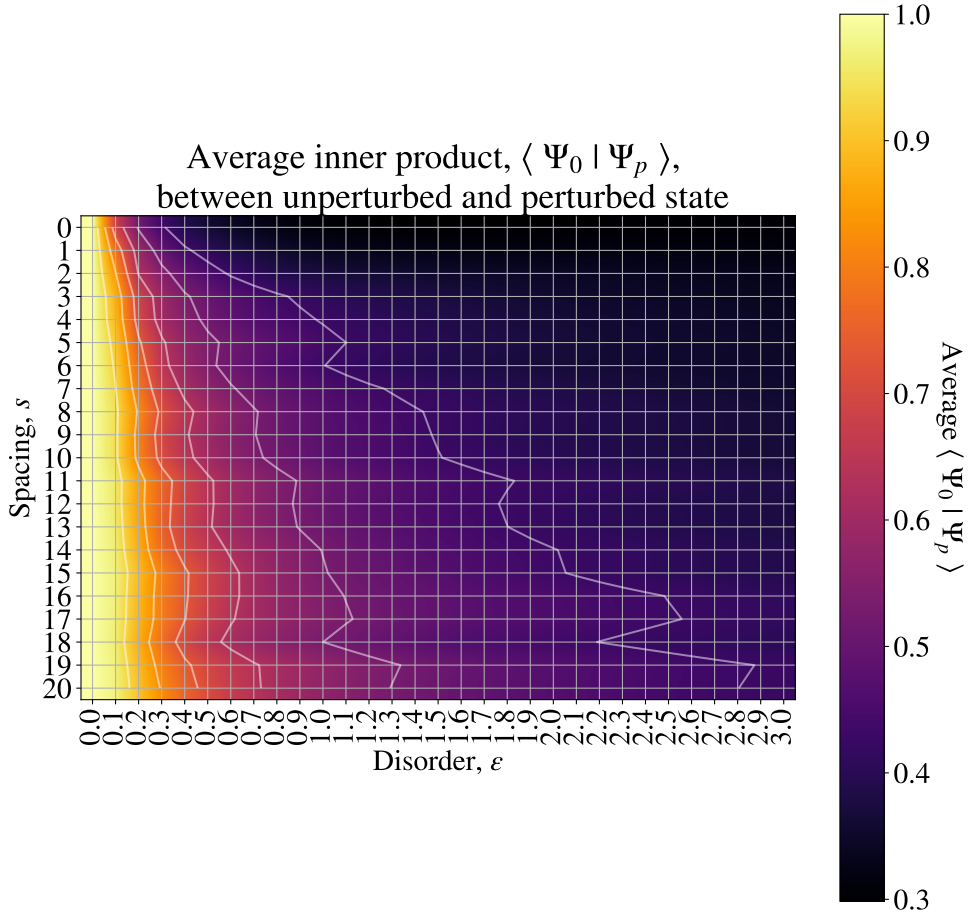

Figure 5: Average inner product $\langle \Psi_0(T) | \Psi_p(T) \rangle$ plotted against disorder amplitude and spacing. As spacing decreases, and as disorder increases, the inner product decreases.

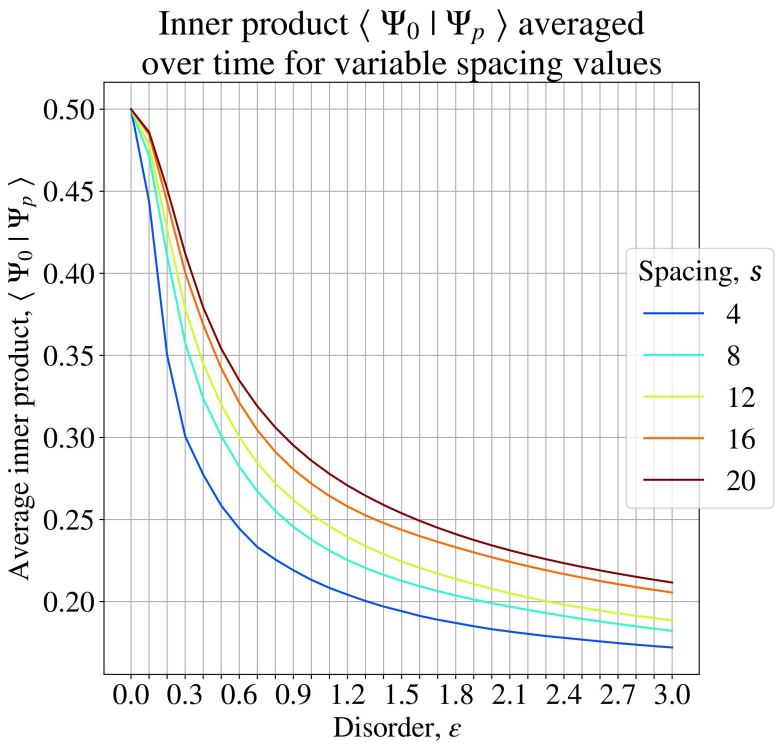

Figure 6: Analysis of the inner product $\langle \Psi_0(t) | \Psi_p(t) \rangle$ averaged over all time steps for variable spacing, s, and disorder, ε. We see the same phenomenon as in Figure 5, where decreasing the spacing and increasing the disorder causes the inner product to decrease.

4 Conclusions and final remarks

In the numerical example in section 2, the Anderson localisation of the wave packet emerges as a result of the interference between the reflected and transmitted waves by the array of step barriers. The effect of the array of barriers generates the confinement of the wave packet in finite region of the space as we can see in Figure 2. The length of the localisation region decreases as the maximal value of the amplitude of the potential barriers ε is increased.

For the harmonic oscillator perturbed with a series of random barriers, it is possible to observe the same kind of localisation effect around the minimum of the potential when the wave packets are initialised at this minimum. The transport in the disordered medium is less than the transport in the unperturbed version of the system. For some critical values of the noise parameters the wave function is almost localised on the minimum of the harmonic oscillator potential.

The effects of the disorder have a clear impact on the evolution of the wave packet. Figures 4, 5 and 6 show the scalar product $\langle \Psi_0(x,t) | \Psi_p(x,t) \rangle$, comparing the evolution of the wave packet in the disordered media with the evolution in harmonic oscillator. Changes in the parameters of the disorder ε and s manifest in the evolution of the system.

5 Acknowledgements

The author would like to acknowledge the bursary award for summer projects from the School of Mathematics of Bristol University and the financial support provided by the EPSRC Grant No. EP/P021123/1.

Appendices

A The Crank-Nicolson method

The Crank-Nicolson method combines the forward and backward Euler methods [6] for solving differential equations - in our case, the one dimensional, time-dependent Schrödinger equation:

$$\left(\frac{-h^2}{2m} \frac{d^2}{dx^2} + V(x) \right) \Psi(x,t) = i\hbar \frac{\partial}{\partial t} \Psi(x,t). \tag{10}$$

Written in operator form, this looks like:

$$\widehat{H}\Psi(x,t) = i\frac{\partial \Psi(x,t)}{\partial t}, \tag{11}$$

where we have also taken $\hbar = 1$. The forward Euler method is explicit and hence offers us relatively less computational expense when compared with the backward Euler method, which is implicit. However, due to its explicit nature, we find the backward Euler method to be more computationally stable. This leads us to combine the two, yielding the so-called Crank-Nicolson method, which offers us greater stability for less computational strain.

Our employment of the Crank-Nicolson method looks like this:

$$\frac{\Psi(x,t+dt) - \Psi(x,t)}{dt} \approx \frac{\widehat{H}}{2i} \left(\Psi(x,t) + \Psi(x,t+dt) \right),$$

and can be rearranged for $\Psi(x,t)$ to give us:

$$\Psi(x,t+dt) = \left(1 - \frac{\widehat{H}dt}{2i}\right)^{-1} \left(1 + \frac{\widehat{H}dt}{2i}\right) \Psi(x,t), \tag{12}$$

assuming that $\widehat{H}$ is invertible.

Calculating the inverse matrix $\widehat{H}$ is computationally very expensive. For this reason we make use of the second order finite difference approximation in order to discretise our continuous variable x into N 'sites' x_i, and hence reduce $\widehat{H}$ to a tri-diagonal matrix. This makes computer simulation feasible whilst allowing us to recover continuity in the limit $N \to \infty$. To be explicit, this gives us a Hamiltonian operator, $\widehat{H}$, of the form:

$$\widehat{H} = \frac{1}{2}\begin{pmatrix} 2 & -1 & & \\ -1 & 2 & -1 & \\ & -1 & 2 & -1 \\ & & & \ddots \end{pmatrix} + \begin{pmatrix} V(0) & & & \\ & V(1) & & \\ & & V(2) & \\ & & & \ddots \end{pmatrix}. \tag{13}$$

The Hamiltonian will be an NxN matrix, with each $V(i)$ being the value of the potential at a given x_i, where $i \in 0, ..., N-1$. This can be seen in the project code, which is found by following the link in appendix B.

B Code

The online repository with code for the calculations is in:
`https://github.com/emgsharp99/evolution-DQS`

References

[1] Mattia Walschaers, Frank Schlawin, Thomas Wellens, and Andreas Buchleitner. Quantum transport on disordered and noisy networks: An interplay of structural complexity and uncertainty. *Annual Review of Condensed Matter Physics*, 7(1):223–248, 2016.

[2] P. W. Anderson. Absence of diffusion in certain random lattices. *Phys. Rev.*, 109:1492–1505, Mar 1958.

[3] Ad Lagendijk, Bart van Tiggelen, and Diederik S. Wiersma. Fifty years of Anderson localization. *Physics Today*, 62(8):24–29, 2009.

[4] M. Díaz, P. A. Mello, M. Yépez, and S. Tomsovic. Wave transport in one-dimensional disordered systems with finite-width potential steps. *EPL (Europhysics Letters)*, 97(5):54002, mar 2012.

[5] A.F.J. Levi. *Applied Quantum Mechanics*. Cambridge University Press, second edition, 2012.

[6] Michael Zeltkevic. Forward and backward Euler methods. `https://web.mit.edu/10.001/Web/Course_Notes/Differential_Equations_Notes/node3.html`, Apr 1998.